

Fed-batch growth of *Rhizopus oryzae*: eliminating ethanol formation by controlling glucose addition

Nicolaas W. de Jongh, Reuben M. Swart, Willie Nicol*

Department of Chemical Engineering, University of Pretoria, Lynnwood Road, Hatfield,
0002, Pretoria, South Africa

Bioreaction Engineering Research Group¹,

Abstract

Rhizopus oryzae is a prominent strain for producing fumarate, where biomass growth precedes fumarate production. The natural biofilm growth of *R. oryzae* as fungal mat was investigated using different glucose addition strategies in a novel fed-batch fermenter. Batch growth was compared through three fed-batch runs, each with a different glucose addition strategy. The fed-batch runs involved a constant glucose feed (CGF) of 0.075 g h^{-1} and controlled glucose feeds in order to keep the respiration quotient (RQ) at either $1.3 \text{ mol CO}_2 \text{ mol}^{-1} \text{ O}_2$ (RQ1.3) or $1.1 \text{ mol CO}_2 \text{ mol}^{-1} \text{ O}_2$ (RQ1.1). Ethanol overflow via the established Crabtree mechanism was completely negated for the CGF and RQ1.1 runs, while the batch and RQ1.3 runs exhibited significant ethanol formation. Biomass yield on glucose was found to be 0.476 g g^{-1} (RQ1.1), 0.194 g g^{-1} (RQ1.3), 0.125 g g^{-1} (CGF) and 0.144 g g^{-1} (batch). The results indicate a three-fold improvement in biomass yield when comparing the batch run with the RQ1.1 run. In addition, the RQ1.1 run resulted in zero detectable byproducts, unlike the batch scenario where pyruvate and fumarate were associated with ethanol formation. Clear evidence is provided that glucose overflow can be fully eliminated during *R. oryzae* growth, significantly affecting the biomass yield on glucose.

*Prof. Willie Nicol

Email address: willie.nicol@up.ac.za (Bioreaction Engineering Research Group)

Key words: *Rhizopus oryzae*, respiration quotient, controlled substrate addition, Crabtree effect, fumarate production, fed-batch reactor

1. Introduction

The dicarboxylic acids of the tricarboxylic acid (TCA) cycle, namely malate, fumarate and succinate, are important biobased intermediates for the production of various bulk-scale chemicals [1]. These three acids are structurally similar with malate and succinate respectively being only a hydration and hydrogenation step away from fumarate. Due to its double bond, fumarate is the most diverse intermediate of the three, as it is more economically feasible to add chemically, rather than remove, H_2 and H_2O . In addition, fumarate is a single dehydration reaction away from maleic anhydride, which has a market size of approximately 4.36 billion USD (2025 projection) [2]. Fumarate in its acid form also has a very low solubility in water (4.3 g l^{-1} at $15\text{ }^{\circ}\text{C}$) [3] which significantly simplifies downstream processing from the fermenter.

Nomenclature

ADH	alcohol dehydrogenase
ATCC	American Type Culture Collection
CGF	constant glucose feed addition fed-batch experiment
CSIR	Council for Scientific and Industrial Research
HPLC	high-performance liquid chromatography
MRM	metabolic regime map
PI	proportional-integral
R^2	coefficient of determination
RI	refractive index
RQ	respiration quotient
RQ1.1	fed-batch experiment with RQ kept at 1.1
RQ1.3	fed-batch experiment with RQ kept at 1.3
RSD	relative standard deviation
SCDA	short-chain dicarboxylic acid
TCA	tricarboxylic acid

Fumarate has a vast range of applications. It is used in the treatment of psoriasis [4] and multiple sclerosis [5]. Piglets [6], broilers [7] and cattle [8] are fed fumarate to reduce emissions of greenhouse-associated methane. Fumaric acid tastes more acidic than citric acid on a mass basis (1.36 g of citric acid to every 0.91 g of fumaric acid) and is suitable for use as a food acidulant [9]; it is also used as solid state acid in baking soda [10]. A high extent of cross-linking results when fumarate is utilised in the industrial production of polyester resins [11]. Fumarate has been shown to produce small pore sizes in the production of metal-organic frameworks for advanced electrochemical energy storage devices [12]. For more applications of fumarate consult the paper by Doscher et al. [13].

The biological production of fumaric acid is mostly associated with the *Rhizopus* fungal genus. *Escherichia coli* has been manipulated to produce fumarate in small quantities [14], but the results are far from those obtained in promi-

ment *Rhizopus* fermentations. *Rhizopus oryzae* (ATCC 20344, also referred to as *Rhizopus delemar* [15]) is one of the most prominent and studied *Rhizopus* species for producing fumarate, with the titres obtained being between 25 g l⁻¹ [16] and 103 g l⁻¹ [17] and the productivities between 0.19 g l⁻¹ h⁻¹ [18] and 1.21 g l⁻¹ h⁻¹ [19]. Genetic modifications of *R. oryzae* have been proved to result in minor fermentation improvements [16]. The paper by Sebastian et al. [20] is a useful reference for comparative fumarate fermentations.

Depending on the desired product, different medium compositions and reactor setups are utilised when fermenting with *R. oryzae*. Examples include introducing plant hormones into a whey medium for enhanced growth and chitosan production [21] and utilising *R. oryzae* cells immobilised within biomass support particles as a whole-cell biocatalyst for the production of biodiesel fuel from plant oils [22]. For targeted fumarate production, ethanol coproduction presents the most prominent challenge [23]. Ethanol as byproduct increases downstream separation costs and wastes valuable feedstock materials by decreasing the yield. Numerous strategies have been employed to minimise ethanol coproduction, such as mutation and the selection of strains with less-active ethanol-producing metabolic pathways [24] [25] and overexpressing native mitochondrial fumarase [26]. Oxygen availability plays a major role in the wastewater treatment process, where airlift bioreactors [27] and membrane bioreactors [28] may be used for uniform aeration and filtration of oxygen consuming heterotrophic bacteria, respectively. Similarly, ethanol production by *R. oryzae* is conventionally viewed as a result of insufficient availability of oxygen during fermentation. Numerous studies attempt to increase the availability of cell oxygen by inducing biomass pelletisation in flasks, stirred tank reactors and airlift bioreactors [29] [30] [31] [32] [33] . Mycelial cotton-like floc formation [34] using woven towel [35] and honeycomb matrix [36] growth scaffolding as well as vigorous shaking during solid state fermentation also increases the cellular surface area for oxygen uptake. None of these attempts at improving oxygen availability have resulted in the elimination of ethanol coproduction. In a recent paper by Swart et al. [37] it was clearly illustrated that *R. oryzae* is a Crabtree-positive organism.

This implies that ethanol production is a result of an overflow mechanism by which excessive glucose uptake is channelled into ethanol. The work showed that ethanol production can be completely avoided by manipulating the glucose availability in the fermenter.

The study by Swart et al. [37] employed the fermenter design developed by Naude et al. [38] [39] [40]. In this fermenter biomass is **naturally** immobilised on both sides of a polypropylene **tube, utilising shear force generated by the liquid recycle flowrate. The medium was agitated by high flowrate recycling of the fermentation broth from the inside to the outside of the polypropylene growth scaffold and alternating flow direction every 2 min to prevent biomass tube clogging.** The thickness of the attached fungal mat is controlled by the amount of glucose supplied for the growth part of the fermentation. The immobilised biomass enables the fast replacement of the fermentation medium without removing any biomass. During this process the spent growth medium can be replaced with a nitrogen-lean production medium so that fumarate excretion is the major metabolic flux. The setup is also supplied with an off-gas analyser of oxygen and carbon dioxide that enables real-time analysis of fermentation fluxes. Most of the studies on this fermenter have focused on the fumarate production phase, where a nitrogen-lean medium is employed to enforce fumarate excretion [38] [39] [40] [37].

The current study focused only on the growth phase of the fumarate fermentation. The objective was to maximise the yield of biomass on glucose by eliminating byproducts other than respiratory carbon dioxide. The paper by Swart et al. [37] has clearly proved that *R. oryzae* is a Crabtree-positive organism similar to *Saccharomyces cerevisiae* [41]. Production of *S. cerevisiae* biomass is commonly associated with the control of glucose availability. The strategy employed is to manipulate the cellular uptake of glucose and to eliminate the aerobic formation of ethanol. Ethanol formation in Crabtree-positive organisms is a result of the glucose uptake rate which exceeds the glucose flux that can be processed by the mitochondria of the eukariotic cell [37]. The surplus of intracellular glucose is accordingly channelled to ethanol (often described

as an overflow) whereby additional cellular energy is obtained [41]. To avoid ethanol overflow a fed-batch fermenter is employed where the feed rate is adjusted as the biomass content in the fermenter increases. The objective of the glucose feeding is to maintain a cellular glucose uptake rate less than or equal to the glucose flux that the respiration system can process [42] [43]. Overfeeding of glucose results in the formation of ethanol and this can be observed in the off-gas product, with an increase in carbon dioxide content due to its co-formation with ethanol [44]. A similar fed-batch strategy of eliminating the overflow metabolism of Crabtree-positive organisms was attempted by Habegger et al. [45] by controlling the organism specific growth rates of *S. cerevisiae* and *Escherichia coli*, respectively. Here biomass concentration was measured online via dielectric spectroscopy and turbidity measurements and glucose was fed according to a feedforward-feedback control scheme. This approach and controller algorithm was later refined on *Kluyveromyces marxianus* [46]. A root mean square specific growth rate control error of $23 \pm 6\%$ is reported by Brignoli et al. using an optimised novel proportional-integral (PI) feedforward-feedback controller with a first order Savitzky–Golay noise filter algorithm [46]. Butkus et al. also proposes a fuzzy logic-based strategy for specific growth rate adaptive control of *E. coli* [47].

This paper explores the concept of ethanol free biomass production for *R. oryzae*. A batch fermentation with excess glucose provides the baseline for improving the growth yield on glucose. Subsequently various fed-batch strategies are employed in order to reduce the formation of ethanol and other byproducts. The first fed-batch run employed a constant glucose feed (CGF), while the other runs used the off-gas ratio of carbon dioxide to oxygen (respiration quotient or RQ) to alter the glucose feed during the fermentation. Two different setpoint values of RQ were investigated.

2. Experimental

2.1. Microorganism and culture conditions

R. oryzae (ATCC 20344) obtained from the Spanish collection of cultures (Colección Española de Cultivos Tipo, Valencia, Spain) was prepared as described previously by Naude and Nicol [38]. Cultures were grown on potato dextrose agar plates for 96 h at 35 °C to induce spore production. Plates were stored at 4 °C after adequate sporulation for no longer than two weeks, before being discarded. Spores were separated from the plates by washing with distilled water and hydrated at 25 °C for 12 h without agitation before being injected. Spore concentrates were checked for infections by inoculating a growth medium similar to the reaction medium at 35 °C and testing for any unknown or infection-indicative metabolites via high performance liquid chromatography (HPLC) analysis. The inoculum consisted of a 10 ml solution containing 8×10^6 spores ml^{-1} . Any variation in inoculum size or spore concentration was mitigated by defining an experimental starting point immediately after 2 g of glucose was consumed batchwise.

2.2. Medium

The composition of the experimental growth medium is presented in Table 1.

Table 1: Growth medium composition.

Compound	Batch (g l^{-1})	Fed-batch init. (g l^{-1})	Fed-batch washed (g l^{-1})
Glucose	6	2	0
Urea	2	2	2
KH_2PO_4	0.6	0.6	0.6
$\text{MgSO}_4 \cdot 7\text{H}_2\text{O}$	0.25	0.25	0.25
$\text{ZnSO}_4 \cdot 7\text{H}_2\text{O}$	0.088	0.088	0.088
$\text{FeSO}_4 \cdot 7\text{H}_2\text{O}$	0.0005	0.0005	0.0005

The fed-batch glucose feed concentration was 100 g l^{-1} . Medium components were sourced from Merck (South Africa). All medium solutions were prepared with distilled water and sterilised at 121°C for 1 h in an autoclave. Glucose, urea, sulphates and phosphates were sterilised in separate containers and combined once they had cooled to room temperature to prevent irreversible mineral precipitation reactions from occurring while at high temperatures.

2.3. Fermentation

The in-house designed and locally produced novel reactor used was a modified version of that used by Naude and Nicol [38]. The setup process flow diagram may be found in Appendix A, presented in Fig. A.5. The reaction liquid volume was 1 l with a gas phase volume of 0.3 l. The polypropylene growth scaffold had a length of 386.5 mm and outer and inner diameters of 40 mm and 32 mm respectively. A 79% N_2 /21% O_2 Afrox instrument-grade synthetic air mixture and Afrox instrument grade CO_2 were sparged through the reactor via Brooks GF40 mass flow controllers at flowrates of 90 ml min^{-1} and 10 ml min^{-1} respectively. Atmospheric pressure was 86 kPa. Liquid temperature was controlled and kept constant at 35°C . Initial medium pH at inoculation was at 6.5. As organic acids were produced during batch fermentations, the pH was controlled, by dosing 10 M NaOH, to not drop below 5.0. As little to no acids were produced during fed-batch fermentations, the pH remained relatively constant, but was not controlled, at the initial value of 6.5.

2.4. Growth strategies

A 6 g glucose, 2 g urea and mineral-containing medium 1 was batch fermented with *R. oryzae* until full glucose depletion. All attempts at growth strategy improvement were fed-batch experiments. An initial amount of biomass, referred to as starter biomass, was grown batchwise with 2 g of glucose in the medium before the immobilised cells, as part of a naturally produced fungal mat biofilm on a scarred polypropylene tube, were washed twice with a mineral solution, and the glucose feed strategy was initiated for each respective fed-batch

run, feeding 4 g of glucose over time. The same total amount of 6 g glucose was consumed in the batch experiment and all fed-batch experiments. The yield results of biomass on glucose were compared with respect to the biomass produced from the fed 4 g glucose and the corresponding consumed 4 g glucose in the respective fed-batch and batch experiments.

The cellular ethanol production rate was controlled by altering the glucose addition rate. Effluent gas composition was measured online, enabling instantaneous feed rate manipulation, controlling the RQ. A proportional-integral (PI) controller was implemented for this purpose, keeping organism RQ at 1.3 and 1.1 for experiments RQ1.3 and RQ1.1, respectively. Glucose was fed at a constant rate of 0.075 g h^{-1} for experiment CGF.

The glucose feed rate controller output was determined by:

$$r_S^{feed} = K_P * (e + \frac{1}{T_I} I_{term}) \quad (1)$$

where r_S^{feed} is the glucose feed rate, K_P is the proportional gain constant, e is the error value: the difference between the controlled variable set point and measured value, T_I is the integral time constant, and I_{term} is the current accumulative integral term. The current accumulative integral term was calculated by:

$$I_{term} = I_{term}^{t-1} + e \quad (2)$$

where I_{term}^{t-1} is the accumulative integral term calculated from the start of controlled feed initiation up until the previous measurement time (previous second). The error was calculated as:

$$e = SP - RQ_{meas} \quad (3)$$

where SP is the controlled variable set point and RQ_{meas} is the controlled variable (RQ) measured value passed through a 10 min simple moving average filter.

2.5. Analytical methods

The concentration of the liquid metabolites: glucose, ethanol, fumarate, malate, pyruvate and glycerol were measured via high performance liquid chro-

matography (HPLC) with an Aminex HPX-87H ion exchange column (Bio-Rad Laboratories, USA) equipped with a refractive index (RI) detector (55 °C) and a 300 mm \times 7.8 mm Aminex HPX-87H ion-exchange column (Bio-Rad Laboratories, USA). Standard curves for these compounds were generated by plotting the area under the resulting peaks against known concentration values before fitting a straight line through the origin and at least two other known points. Standard concentration and coefficient of determination (R^2) values for each compound is provided in Table 2.

Table 2: HPLC standard concentration and coefficient of determination R^2 values for glucose, ethanol, fumarate, malate, pyruvate and glycerol.

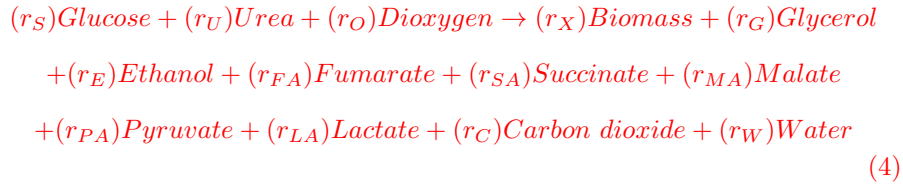
Compound	Conc. (g l^{-1})	R^2	Compound	Conc. (g l^{-1})	R^2
Glucose	0.1001	1.00000	Malate	0.1099	1.00000
	1.001			1.099	
	10.01			10.99	
Glycerol	0.1009	0.99988	Pyruvate	0.1021	0.99997
	1.009			1.021	
	10.09			10.21	
Fumarate	0.1039	0.99587	Ethanol	0.9898	1.00000
	1.039			9.898	

Both mobile phase (phase A: $1.95 \text{ g l}^{-1} \text{ H}_2\text{SO}_4$, phase C: 0.53 g l^{-1}) flowrates were 0.6 ml min^{-1} with a column temperature of $60 \text{ }^\circ\text{C}$ as previously described by Naude and Nicol [38]. The reactor mixed-phase effluent was separated into gas and liquid phases. The liquid phase was discarded and the gas phase composition analysed online. A Tandem Gas Analyser (Magellan Biotech, UK) was used to measure effluent gas CO_2 and O_2 concentrations as previously described by Naude and Nicol [38]. Reactor steady-state gas composition was determined before culture inoculation and used as a baseline for zero metabolic gas activity. Immobilised biomass on the polypropylene growth scaffold was removed,

washed, dried and weighed as previously described by Naude and Nicol [38].

2.6. Mass balance checks and repeatability

The metabolic map for *R. oryzae* is provided and discussed by Naude and Nicol [38] and may be mathematically described by performing a mass balance over the system with the following overall reaction taking place:



with each respective r_i denoting the volumetric reaction rate of the corresponding compound in $\text{cmol l}^{-1} \text{h}^{-1}$. Elemental balances were done for C, H, O and N over the entire fermenter. In addition, all metabolite rate values were measured, except those of water and biomass production. The system may be fully described with 13 equations, but 10 specifications were already available (discounting biomass and water) along with the four elemental balances, thus leaving one overspecification. This additional specification was utilised to quantify gross measurement errors graphically through data reconciliation. No significant errors were observed.

Starter biomass values from 2 g glucose batch fermentations were obtained from three separate experiments and are presented in Table 3.

Table 3: Starter biomass values from 2 g glucose batch fermentations. Calculated relative standard deviation (RSD) to the average.

Starter biomass (g)	
Experiment 1	0.542
Experiment 2	0.549
Experiment 3	0.613
Average	0.568
RSD to average	0.056

Three separate batch fermentations were performed, for which liquid metabolite, off-gas, measured final biomass and mass balance **calculated** biomass analysis was performed. The standard deviation is presented via error bars for liquid metabolites and via dashed line profiles for off-gas.

The analysis of time, measured final and mass balance predicted biomass value is presented in Table 4.

Table 4: analysis of time, measured final ($m_X^{measured\ final}$) and mass balance predicted ($m_X^{predicted}$) biomass value. Calculated relative standard deviation (RSD) to the average.

	Time (h)	$m_X^{measured\ final}$ (g)	$m_X^{predicted}$ (g)
Experiment 1	8.5	1.107	1.007
Experiment 2	7.1	1.165	1.161
Experiment 3	8.6	1.164	1.315
Average	8.066	1.145	1.161
RSD to average	0.085	0.024	0.108

3. Results and discussion

A comprehensive kinetic model for *R. oryzae* may be obtained from two previous publication by Naude and Nicol [38] [39].

It is often attempted to manipulate Crabtree-positive organism overflow metabolisms by controlling the respective organism specific growth rate [45] [46] [47]. One major challenge to this approach is accurately estimating the current specific growth rate based on online biomass concentration measurements [45]. Biofilm formation, air-liquid bubble dynamics and changes in medium conductivity caused by the addition of base and feed may produce large measurement inaccuracies, whereas online RQ measurements are independent of these factors and provide for overall far less noisy data. As specific growth rate controller algorithms often contain exponential terms, a sudden change in measured error value may result in an exaggerated controller output, possibly causing system instability. The linear nature of RQ controller algorithms results in a less-exaggerated controller response, thereby aiding system stability.

The RQ provides a direct indication of active metabolic fluxes. When only respiration is considered the RQ will have a value of unity since a mole of CO_2 is formed for each mole of O_2 consumed. Biomass growth is typically associated with the formation of anabolic CO_2 and hence the RQ is expected to be slightly higher than unity when respiration energy is the sole driver for growth. Ethanol formation is caused by high glucose concentrations in the broth, which enhances glucose uptake beyond the respiratory capacity of the cell. Since ethanol formation is associated with the coformation of CO_2 , a higher RQ is likely to result if fumarate formation is small or negligible (fumarate formation is associated with the uptake of CO_2 , which would reduce the RQ). Controlling the RQ via feed manipulation thus implies that the flux distribution within the cell is controlled. The desired effect of spending glucose on only the organism anabolism and respiration, may only be achieved if a suitable RQ-value range is selected for exploration. If a theoretical batch fermentation is considered as a starting point for RQ-range determination: we would expect the resulting RQ to be higher than what we desire as additional CO_2 is present, originating from significant ethanol formation and some CO_2 being consumed during fumarate

production. The theoretical desired RQ may be described as:

$$RQ^{desired} = \frac{r_C^X + r_{resp}}{r_O^{tot}} \quad (5)$$

where $RQ^{desired}$ is the desired RQ at which only biomass production and respiration takes place in mol mol^{-1} , r_O^{tot} is the total O_2 consumption rate in $\text{mol l}^{-1} \text{h}^{-1}$, $r_C^{r_{resp} + X}$ is the rate at which CO_2 , originating from only biomass production and respiration, is produced in $\text{mol l}^{-1} \text{h}^{-1}$, calculated by:

$$r_C^{X + resp} = r_C^{tot} + r_C^{FA} - r_C^E \quad (6)$$

where r_C^{tot} is the total CO_2 production rate in $\text{mol l}^{-1} \text{h}^{-1}$, r_C^{FA} is the CO_2 consumption rate during fumarate production in $\text{mol l}^{-1} \text{h}^{-1}$ and r_C^E is the CO_2 production rate during ethanol production in $\text{mol l}^{-1} \text{h}^{-1}$. The liquid metabolite dependant CO_2 rates, r_C^{FA} and r_C^E may be determined as:

$$r_C^{FA} = 0.25r_{FA} \quad (7)$$

and

$$r_C^E = 0.5r_E \quad (8)$$

where r_{FA} is the fumarate production rate in $\text{cmol l}^{-1} \text{h}^{-1}$ and r_E is the ethanol production rate in $\text{cmol l}^{-1} \text{h}^{-1}$. A suitable variance may then be selected around $RQ^{desired}$ for experimental exploration. According to the metabolic map of *R. oryzae*, if only respiration is considered, every mole of CO_2 produced requires one mole of O_2 to be consumed; resulting in a theoretical minimum organism RQ of 1.0 mol mol^{-1} . Maximum RQ is achieved under batch conditions (Fig. 2a) with an average value of 1.901 mol mol^{-1} . Analysis of the batch liquid and gas metabolite rate profiles reveals that the ideal RQ-value where only biomass production and respiration occurs lies approximately between 1.0 and 1.3.

Fig. 1 displays the liquid metabolite concentrations for the batch and fed-batch runs.

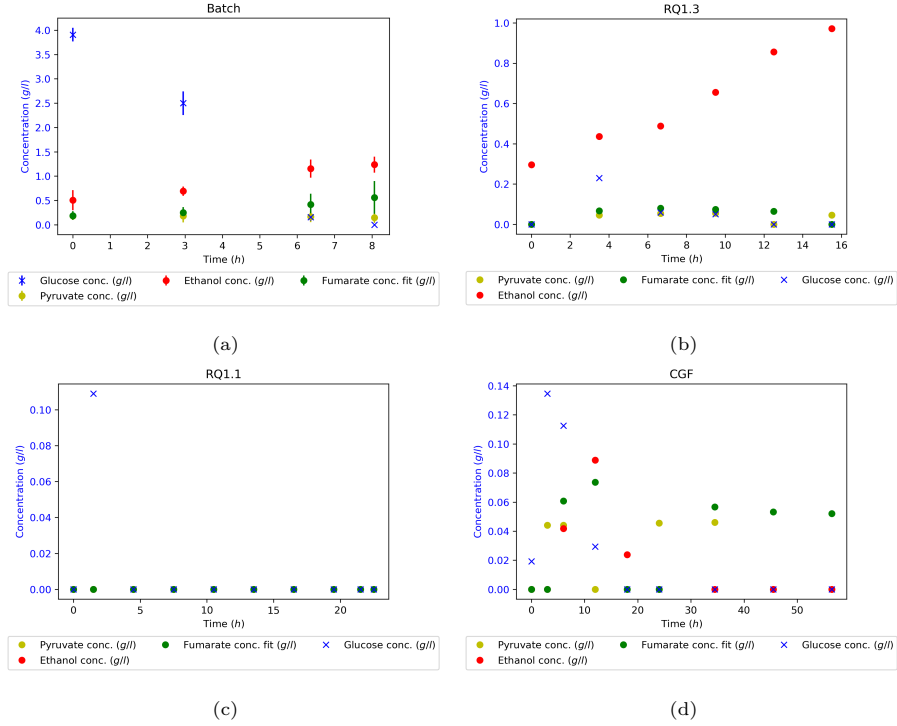


Figure 1: Liquid metabolite analyses of a) batch, b) RQ1.3, c) RQ1.1, d) CGF. Ethanol production was observed for batch and RQ1.3, but not RQ1.1 and CGF. In addition to ethanol, significant amounts of pyruvate and fumarate were also produced during the batch experiment. Three batch experiments were performed, where error bars represent the standard deviation.

The glucose consumption profile for the batch run follows a typical exponential trend. Significant amounts of ethanol and organic acids can be seen as a result of the high prevailing glucose concentrations during the batch run. Ethanol overflow is also clearly observed for the fed-batch run where the RQ was controlled at a value of 1.3. The fermentation time for the RQ1.3 run is double that of the batch run (see Table 5), indicating that the glucose flux was restricted in this run. Nevertheless, the glucose uptake restriction was not sufficient to negate ethanol formation. It can, however, be observed that the formation of fumaric acid is less than that of the batch run. For the RQ1.1 run it is clear that the overflow of ethanol and organic acids is completely eliminated,

indicating that respiration was the only catabolic pathway. Note the longer fermentation when comparing RQ1.1 with RQ1.3 (also see Table 5), indicating that the glucose uptake rates were lower for RQ1.1. The constant glucose feed run (CGF) took much longer than all the other runs due to the fact that the glucose addition flowrate was not increased as biomass accumulated. Apart from small amounts of ethanol formation at the start of the run (at higher glucose concentrations), ethanol overflow was absent, as was expected from the low glucose uptake. Small amounts of organic acid excretion were observed in this run, unlike the RQ1.1 run where no organic acids could be detected.

Table 5: Experiment duration with corresponding biomass productivities and approximate average RQ values.

	Time (h)	Prod. ($\text{mg l}^{-1} \text{ h}^{-1}$)	Avg. RQ (mol mol^{-1})
batch	8.066	142.0	1.901
CGF	56.50	18.87	1.074
RQ1.3	15.50	86.74	1.281
RQ1.1	22.50	109.9	1.069

The composition of the reactor effluent gas stream was analysed for all experiments. Glucose, O_2 consumption and CO_2 production rates, as well as RQ are presented in Fig. 2.

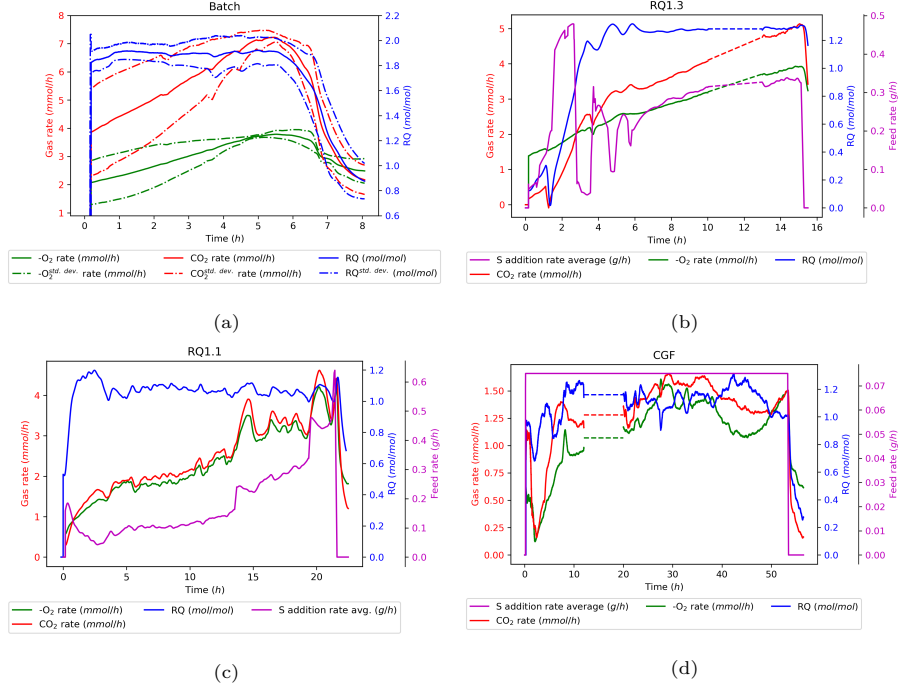


Figure 2: Gas analyses of a) batch (3 runs) , b) RQ1.3, c) RQ1.1, d) CGF. A volumetric rate increase of gas and glucose over time, due to biomass growth, was observed in all runs except CGF. Dashed lines represent a graphical estimate of missing data due to gas analyser malfunction in the RQ1.3 and CGF runs. Three batch experiments were performed, with the dash-dotted lines representing the standard deviation.

For both the runs where the RQ was controlled the O_2 and CO_2 rates follow an increase with time as biomass accumulates. For the batch runs (performed in triplicate) the rate increase is also observed until a sudden drop occurs. This drop can be attributed to the depletion of the available glucose. For the CGF run the O_2 consumption and CO_2 production rates remain more constant, as expected.

The metabolite results from Fig. 1 clearly indicate that the RQ1.1 run was sufficient in negating ethanol formation. The slightly larger amount of CO_2 produced compared with O_2 consumed can be attributed to the formation of anabolic CO_2 and it is safe to deduce that respiration was the only form of cellular ATP generation. For the RQ1.3 run ethanol formation contributed

to ATP generation as can clearly be seen in Fig. 1. In this run glucose was consumed faster than in the RQ1.1 run but slower than in the batch run. The RQ control for the RQ1.3 run was slightly less efficient than that of the RQ1.1 run, mainly due to the glucose overshoot at the start of the fermentation. From Fig. 2 it is clear that tight RQ control is only achieved after 6 hours and it is evident that ethanol formation continues beyond this time (Fig. 1). The faster rate of glucose addition in RQ1.3 allows for a faster cellular glucose uptake and hence the respiration capacity of the cell is exceeded, causing ethanol overflow.

Biomass yields are reported in Fig. 3.

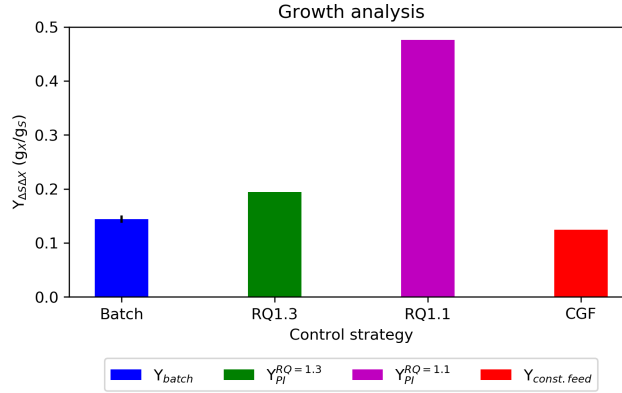


Figure 3: The biomass yield results for the four growth strategies. Calculated yields do not include starter biomass (first 2 g of glucose). Biomass yield of RQ1.1 is 3.3 times higher than that of the batch run. Three batch experiments were performed, with error bars representing the standard deviation.

Fig. 3 clearly illustrates the advantage of controlling the RQ at the correct value. The biomass amount obtained with run RQ1.1 is 3.3 times higher than that of the batch run, while the RQ1.3 run results in a yield between that of the batch and RQ1.1 runs. More biomass is to be expected for the RQ1.1 run since all glucose is channelled to either biomass or respiratory CO_2 . For the batch run the amount of metabolites (excluding CO_2) added up to a value of 2.09 g. This clearly indicates the wastage of glucose in the batch run, where ethanol, fumarate and pyruvate effectively removes the carbon that could have been used

in the anabolism. It is interesting to note that the amount of waste metabolites decreases from 2.09 g for the batch run to 1.06 g for the RQ1.3 run. This makes sense given that the carbon uptake rate in the RQ1.3 run was less than that of the batch run. The low biomass yield for the CGF run is unexpected since the glucose uptake rates were even lower than those of the RQ1.1 run.

Mass balance checks can be performed on the system to validate measurements. Given the elemental balances for carbon, hydrogen, oxygen and nitrogen, as well as all the measured rates, the system is overspecified, with one measurement not required to complete the mass balance. An overall mass balance over the entire timespan of each experiment was performed to calculate the theoretical amount of biomass formed using the assumed biomass elemental composition of $\text{CH}_{1.8}\text{O}_{0.5}\text{N}_{0.16}$. Given the overspecification, either the amount of O_2 consumed or the amount of CO_2 produced was emitted from the calculation. The results of the mass balances can be seen in Table 6.

Table 6: Overall mass balance results for the four growth strategies. Due to an overspecified system, either O_2 or CO_2 rates can be used as specification. Biomass relative error values based on O_2 and CO_2 mass balance specifications are denoted by $e_{\text{O}_2 \text{ spec}}^{\text{relative}}$ and $e_{\text{CO}_2 \text{ spec}}^{\text{relative}}$, respectively.

Exp	m_X^{meas} (g)	$m_X^{\text{calc}, \text{O}_2 \text{ spec}}$ (g)	$e_{\text{O}_2 \text{ spec}}^{\text{relative}}$	$m_X^{\text{calc}, \text{CO}_2 \text{ spec}}$ (g)	$e_{\text{CO}_2 \text{ spec}}^{\text{relative}}$
Batch	1.145	1.161	-0.014	1.246	-0.088
RQ1.3	1.344	1.313	0.023	1.682	-0.251
RQ1.1	2.473	2.367	0.043	2.594	-0.049
CGF	1.066	2.098	-0.967	2.116	-0.985

Both the O_2 and CO_2 specifications resulted in similar predictions, hinting at consistency in the measurements. Predictions of the batch, RQ1.1 and RQ1.3 runs were in good agreement with experimental data, with the O_2 -based predictions resulting in a smaller error. For the CGF run both predictions were double that of the measured amount. **Performing a carbon mole balance over the entire reactor system** indicates that a significant fraction of carbon is unaccounted for

in the CGF run.

Fig. 4 shows the accumulative O_2 consumption profiles for the respective runs and also includes the biomass measurements and predictions.

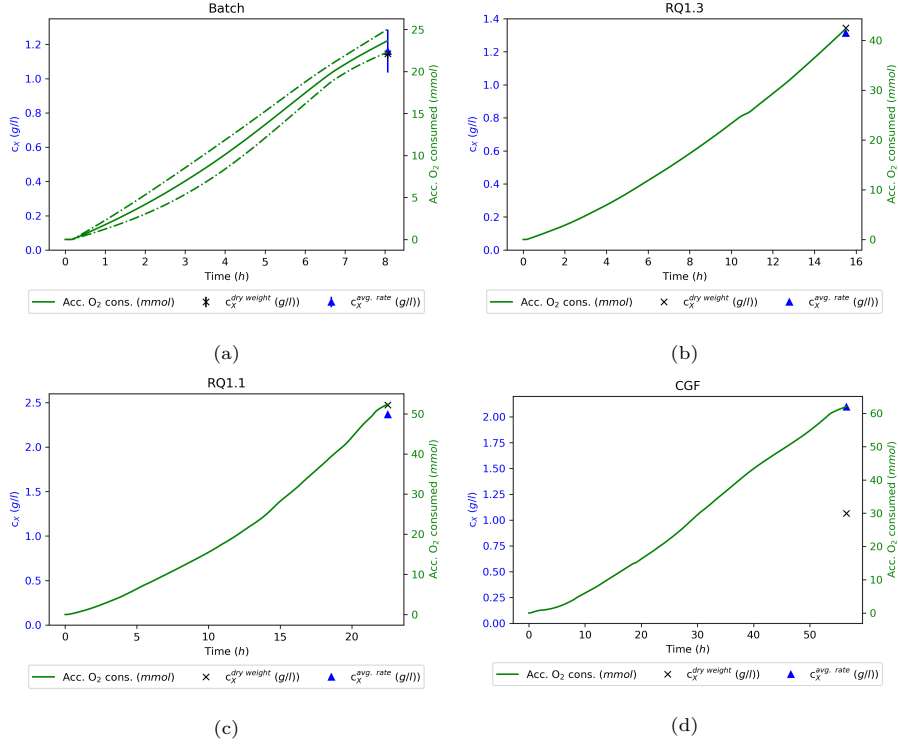


Figure 4: Overall mass balance results for the four growth strategies. Due to an overspecified system either the O_2 or CO_2 rates can be used as specification. Three batch experiments were performed, with error bars and dash-dotted lines representing the standard deviation.

It can be clearly seen that the O_2 usage in the batch fermentation was the smallest. This relates directly to the fact that respiration contributed only partially to generating ATP within the cell. It is interesting to note that the RQ1.1 run, in which only respiration occurred, consumed double the amount of O_2 when compared with the batch run, while the RQ1.3 run resulted in an O_2 consumption between that of the batch and RQ1.1 runs. The CGF feed run consumed more O_2 than the RQ1.1 run and hence the biomass prediction in Table 6 and Fig. 4 is slightly lower. The reason for the very low measured

biomass is unclear. No additional metabolites were observed in HPLC sample analysis of the CGF run, and the total organic carbon (TOC) analysis of the final reactor broth yielded only 15 mg C l^{-1} in the form of non-immobilised cells or proteins, relating to only 0.05 g l^{-1} of biomass when using the assumed elemental composition for biomass.

4. Conclusion

Rhizopus oryzae was grown successfully without ethanol as byproduct. A slow feed addition strategy was employed, by which the feed rate was used to control the RQ via a PI controller. Controlling the RQ at a value of 1.1 eliminated the formation of all unwanted catabolites and resulted in a biomass yield more than three times higher than that of the batch run. It is evident that the Crabtree principle can be used for *R. oryzae* in order to grow biomass at an optimum yield without co-production of any catabolites apart from CO_2 . The results presented contribute to the development of the immobilised *R. oryzae* process, and in addition the growth procedure suggested in this paper will contribute to the improved efficiency of the fumarate production process.

5. Acknowledgements

This work was supported by the University of Pretoria and by the CSIR Inter-bursary Programme, South Africa. Opinions expressed are those of the author and not necessarily attributed to the funding sources. The funding sources were not involved in the study, in the design, in the collection, analysis and interpretation of data, in the writing of the report and in the decision to submit the article for publication.

Appendix A. Reactor setup

A full reactor setup process flow diagram is presented in Fig. A.5.

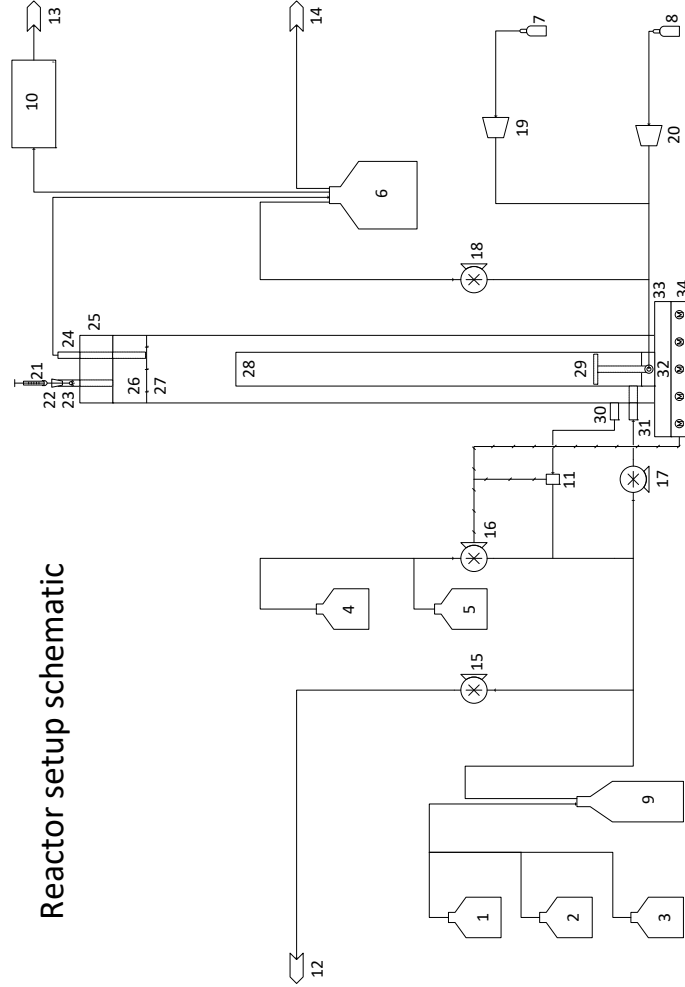


Figure A.5: Experimental setup process flow diagram. 1: Nitrogen (urea), 2: Phosphates, 3: Sulphates, 4: Acid neutraliser (HCl), 5: Base neutraliser (NaOH), 6: Liquid/gas separator, 7: CO₂, 8: Air, 9: Substrate (glucose), 10: Gas analyser, 11: pH and temperature probe, 12: Samples, 13: Gas analyser outlet, 14: Process gas outlet, 15: Sampling pump, 16: Dosing pump, 17: Liquid recycle pump, 18: Gas recycle pump, 19: Gas flow controller (CO₂), 20: Gas flow controller (Air), 21: Syringe, 22: Septum, 23: Inoculation line, 24: Level control line, 25: Reactor cap, 26: Gas space, 27: Liquid space, 28: Growth scaffold, 29: Gas sparger, 30: Outer port, 31: Middle port, 32: Inner port, 33: Reactor base, 34: Heating plate.

References

- [1] T. Werpy, G. Petersen, Top Value Added Chemicals from Biomass, Volume I, US NREL (2004) Medium: ED; Size: 76 pp.[doi:10.2172/15008859](https://doi.org/10.2172/15008859).
URL <http://www.osti.gov/scitech//servlets/purl/15008859-s6ri0N/native/>
- [2] Grand View Research, Maleic Anhydride Market Size, Share & Trends Analysis Report By Application (1,4-BDO, UPR, Additives, Copolymers), By Region (Asia Pacific, North America, Europe, Central & South America, MEA), And Segment Forecasts, 2019 - 2025, Tech. rep. (2019).
URL <https://www.grandviewresearch.com/industry-analysis/maleic-anhydride-market>
- [3] K. Bélafi-Bakó, N. Nemestóthy, L. Gubicza, A study on applications of membrane techniques in bioconversion of fumaric acid to L-malic acid, *Desalination* 162 (1-3) (2004) 301–306. [doi:10.1016/S0011-9164\(04\)00063-3](https://doi.org/10.1016/S0011-9164(04)00063-3).
- [4] U. Mrowietz, E. Christophers, P. Altmeyer, Treatment of severe psoriasis with fumaric acid esters: Scientific background and guidelines for therapeutic use, *British Journal of Dermatology* 141 (3) (1999) 424–429. [doi:10.1046/j.1365-2133.1999.03034.x](https://doi.org/10.1046/j.1365-2133.1999.03034.x).
- [5] S. Schimrigk, N. Brune, K. Hellwig, C. Lukas, B. Bellenberg, M. Rieks, V. Hoffmann, D. Pöhlau, H. Przuntek, Oral fumaric acid esters for the treatment of active multiple sclerosis: An open-label, baseline-controlled pilot study, *European Journal of Neurology* 13 (6) (2006) 604–610. [doi:10.1111/j.1468-1331.2006.01292.x](https://doi.org/10.1111/j.1468-1331.2006.01292.x).
- [6] R. Lan, I. Kim, Effects of organic acid and medium chain fatty acid blends on the performance of sows and their piglets, *Animal Science Journal* 89 (12) (2018) 1673–1679. [doi:10.1111/asj.13111](https://doi.org/10.1111/asj.13111).

- [7] J. Patten, P. Waldroup, Use of organic acids in broiler diets, *Poultry Science* 67 (8) (1988) 1178–1182. doi:10.3382/ps.0671178.
- [8] K. Beauchemin, S. McGinn, Methane emissions from beef cattle: Effects of fumaric acid, essential oil, and canola oil, *Journal of Animal Science* 84 (6) (2006) 1489–1496. doi:10.2527/2006.8461489x.
- [9] P. Shukla, Food additives from an organic chemistry perspective, *MOJ Bioorganic & Organic Chemistry* 1 (3) (2017) 70–79. doi:10.15406/mojboc.2017.01.00015.
- [10] M. Cepeda, R. Waniska, L. Rooney, F. Bejosano, Effects of leavening acids and dough temperature in wheat flour tortillas, *Cereal Chemistry* 77 (4) (2000) 489–494. doi:10.1094/CCHEM.2000.77.4.489.
- [11] G. Rokicki, H. Wodzicki, Waterborne unsaturated polyester resins, *Macromolecular Materials and Engineering* 278 (2000) 17–22. doi:10.1002/(SICI)1439-2054(20000501)278:1<17::AID-MAME17>3.0.CO;2-3.
- [12] A. Baumann, D. Burns, B. Liu, V. S. Thoi, Metal-organic framework functionalization and design strategies for advanced electrochemical energy storage devices, *Communications Chemistry* 2 (1) (2019) 1–14. doi:10.1038/s42004-019-0184-6.
URL <http://dx.doi.org/10.1038/s42004-019-0184-6>
- [13] C. Doscher, J. Kane, G. Cragwall, W. Staebner, Industrial applications of fumaric acid, *Industrial & Engineering Chemistry* 33 (3) (1941) 315–319. doi:10.1021/ie50375a008.
- [14] C. Song, D. Kim, S. Choi, J. Jang, S. Lee, Metabolic engineering of *Escherichia coli* for the production of fumaric acid, *Biotechnology and Bioengineering* 110 (7) (2013) 2025–2034. doi:10.1002/bit.24868.
- [15] A. Abe, Y. Oda, K. Asano, T. Sone, *Rhizopus delemar* is the proper name for *Rhizopus oryzae* fumaric-malic acid producers, *Mycologia* 99 (5) (2007) 714–722. doi:10.3852/mycologia.99.5.714.

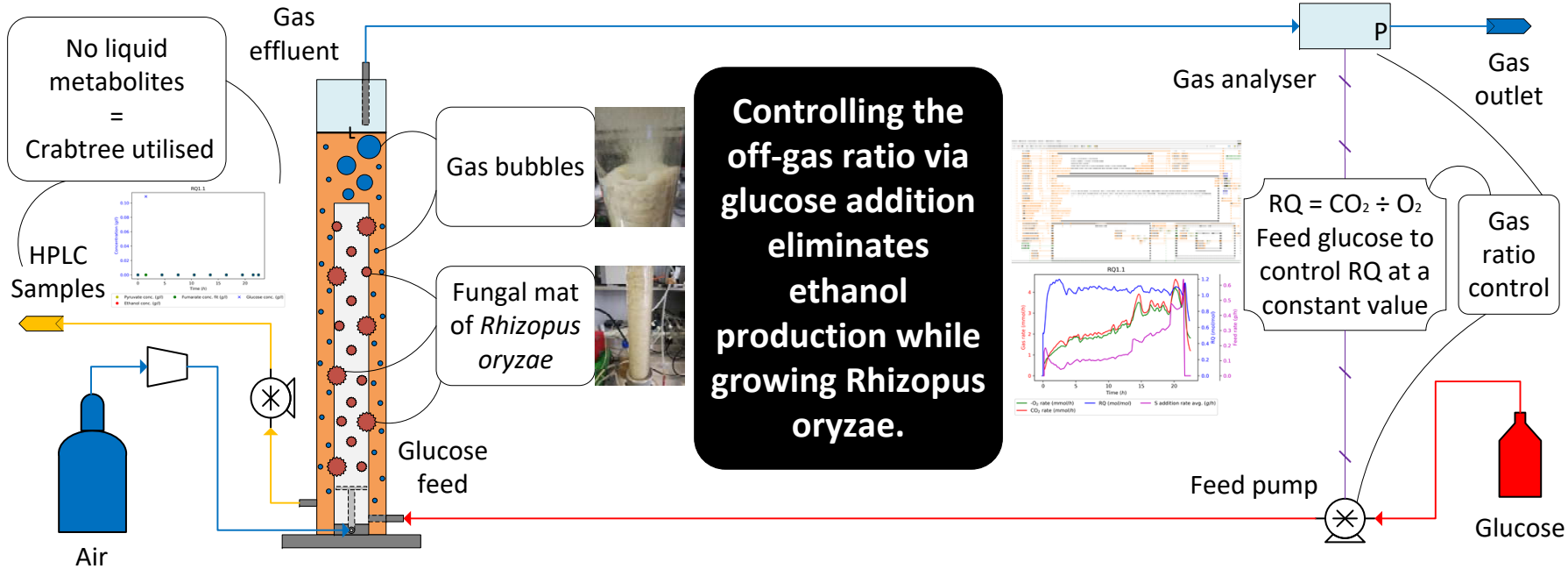
- [16] B. Zhang, C. Skory, S. Yang, Metabolic engineering of *Rhizopus oryzae*: Effects of overexpressing *pyc* and *pepc* genes on fumaric acid biosynthesis from glucose, *Metabolic Engineering* 14 (5) (2012) 512–520. doi:10.1016/j.ymben.2012.07.001.
URL <http://dx.doi.org/10.1016/j.ymben.2012.07.001>
- [17] R. Rhodes, A. Lagoda, T. Misenheimer, M. Smith, R. Anderson, R. Jackson, Production of fumaric acid in 20-liter fermentors, *Applied Microbiology* 10 (1) (1962) 9–15. doi:10.1128/aem.10.1.9-15.1962.
- [18] C. Roa Engel, W. Van Gulik, L. Marang, L. Van der Wielen, A. Straathof, Development of a low pH fermentation strategy for fumaric acid production by *Rhizopus oryzae*, *Enzyme and Microbial Technology* 48 (1) (2011) 39–47. doi:10.1016/j.enzmictec.2010.09.001.
URL <http://dx.doi.org/10.1016/j.enzmictec.2010.09.001>
- [19] R. Das, S. Brar, M. Verma, Enhanced fumaric acid production from brewery wastewater by immobilization technique, *Journal of Chemical Technology and Biotechnology* 90 (8) (2015) 1473–1479. doi:10.1002/jctb.4455.
- [20] J. Sebastian, K. Hegde, P. Kumar, T. Rouissi, S. Brar, Bioproduction of fumaric acid: An insight into microbial strain improvement strategies, *Critical Reviews in Biotechnology* 39 (6) (2019) 817–834. doi:10.1080/07388551.2019.1620677.
URL <https://doi.org/10.1080/07388551.2019.1620677>
- [21] S. Chatterjee, S. Chatterjee, B. Chatterjee, A. Guha, Enhancement of growth and chitosan production by *Rhizopus oryzae* in whey medium by plant growth hormones, *International Journal of Biological Macromolecules* 42 (2) (2008) 120–126. doi:10.1016/j.ijbiomac.2007.10.006.
- [22] K. Ban, M. Kaieda, T. Matsumoto, A. Kondo, H. Fukuda, Whole cell biocatalyst for biodiesel fuel production utilizing *Rhizopus oryzae* cells immobilized within biomass support particles, *Biochemical Engineering Journal* 8 (1) (2001) 39–43. doi:10.1016/S1369-703X(00)00133-9.

- [23] B. Ghosh, R. Rani Ray, Current commercial perspective of *Rhizopus oryzae*: A review, Journal of Applied Sciences 11 (14) (2011) 2470–2486. doi:10.3923/jas.2011.2470.2486.
URL <http://www.scialert.net/abstract/?doi=jas.2011.2470.2486>
- [24] D. Bai, X. Zhao, X. Li, S. Xu, Strain improvement of *Rhizopus oryzae* for over-production of L(+)-lactic acid and metabolic flux analysis of mutants, Biochemical Engineering Journal 18 (1) (2004) 41–48. doi:10.1016/S1369-703X(03)00126-8.
- [25] Y. Fu, Q. Xu, S. Li, Y. Chen, H. Huang, Strain improvement of *Rhizopus oryzae* for over-production of fumaric acid by reducing ethanol synthesis pathway, Korean Journal of Chemical Engineering 27 (1) (2010) 183–186. doi:10.1007/s11814-009-0323-3.
- [26] B. Zhang, S. Yang, Metabolic engineering of *Rhizopus oryzae*: Effects of overexpressing fumR gene on cell growth and fumaric acid biosynthesis from glucose, Process Biochemistry 47 (12) (2012) 2159–2165. doi:10.1016/j.procbio.2012.08.009.
URL <http://dx.doi.org/10.1016/j.procbio.2012.08.009>
- [27] Sepehri, Arsalan and Sarrafzadeh, Mohammad Hossein and Avateffazeli, Maryam, Interaction between *Chlorella vulgaris* and nitrifying-enriched activated sludge in the treatment of wastewater with low C/N ratio, Journal of Cleaner Production 247. doi:10.1016/j.jclepro.2019.119164.
- [28] Sepehri, Arsalan and Sarrafzadeh, Mohammad Hossein, Effect of nitrifiers community on fouling mitigation and nitrification efficiency in a membrane bioreactor, Chemical Engineering and Processing - Process Intensification 128 (December 2017) (2018) 10–18. doi:10.1016/j.cep.2018.04.006.
- [29] D. Bai, M. Jia, X. Zhao, R. Ban, F. Shen, X. Li, S. Xu, L(+)-lactic acid production by pellet-form *Rhizopus oryzae* R1021 in a stirred tank fermentor, Chemical Engineering Science 58 (3-6) (2003) 785–791. doi:10.1016/S0009-2509(02)00608-5.

- [30] W. Liao, Y. Liu, S. Chen, Studying pellet formation of a filamentous fungus *Rhizopus oryzae* to enhance organic acid production, *Applied Biochemistry and Biotechnology* 137 (12) (2007) 689–701.
- [31] Y. Zhou, J. Du, G. Tsao, Mycelial pellet formation by *Rhizopus oryzae* ATCC 20344, *Applied Biochemistry and Biotechnology - Part A Enzyme Engineering and Biotechnology* 84-86 (2000) 779–789. doi:10.1385/abab:84-86:1-9:779.
- [32] P. Yin, K. Yahiro, T. Ishigaki, Y. Park, M. Okabe, L(+)-lactic acid production by repeated batch culture of *Rhizopus oryzae* in air-lift bioreactor, *Journal of Fermentation and Bioengineering* 85 (1) (1998) 96–100. doi:10.1016/S0922-338X(97)80361-3.
- [33] T. Maneeboon, W. Vanichsiratana, C. Pomchaitaward, V. Kitpreechanich, Optimization of lactic acid production by pellet-form *Rhizopus oryzae* in 3-l airlift bioreactor using response surface methodology, *Applied Biochemistry and Biotechnology* 161 (1-8) (2010) 137–146. doi:10.1007/s12010-009-8860-0.
- [34] E. Park, Y. Kosakai, M. Okabe, Efficient production of L-(+)-lactic acid using mycelial cotton-like flocs of *Rhizopus oryzae* in an air-lift bioreactor, *Biotechnology Progress* 14 (5) (1998) 699–704. doi:10.1021/bp9800642.
- [35] N. Chotisubha-Anandha, S. Thitiprasert, V. Tolieng, N. Thongchul, Improved oxygen transfer and increased l-lactic acid production by morphology control of *Rhizopus oryzae* in a static bed bioreactor, *Bioprocess and Biosystems Engineering* 34 (2) (2011) 163–172. doi:10.1007/s00449-010-0457-z.
- [36] Z. Wang, Y. Wang, S. Yang, R. Wang, H. Ren, A novel honeycomb matrix for cell immobilization to enhance lactic acid production by *Rhizopus oryzae*, *Bioresource Technology* 101 (14) (2010) 5557–5564. doi:10.1016/j.biortech.2010.02.064.
URL <http://dx.doi.org/10.1016/j.biortech.2010.02.064>

- [37] R. Swart, F. le Roux, A. Naude, N. de Jongh, W. Nicol, Fumarate production with *Rhizopus oryzae*: Utilising the Crabtree effect to minimise ethanol by-product formation, *Biotechnology for Biofuels* 13 (1) (2020) 1–10. doi:10.1186/s13068-020-1664-8.
URL <https://doi.org/10.1186/s13068-020-1664-8>
- [38] A. Naude, W. Nicol, Fumaric acid fermentation with immobilised *Rhizopus oryzae*: Quantifying time-dependent variations in catabolic flux, *Process Biochemistry* 56 (March) (2017) 8–20. doi:10.1016/j.procbio.2017.02.027.
URL <http://dx.doi.org/10.1016/j.procbio.2017.02.027>
- [39] A. Naude, W. Nicol, Improved continuous fumaric acid production with immobilised *Rhizopus oryzae* by implementation of a revised nitrogen control strategy, *New Biotechnology* 44 (April) (2018) 13–22. doi:10.1016/j.nbt.2018.02.012.
URL <https://doi.org/10.1016/j.nbt.2018.02.012>
- [40] A. Naude, W. Nicol, Malic acid production through the whole-cell hydration of fumaric acid with immobilised *Rhizopus oryzae*, *Biochemical Engineering Journal* 137 (2018) 152–161. doi:10.1016/j.bej.2018.05.022.
URL <https://doi.org/10.1016/j.bej.2018.05.022>
- [41] R. Deken, The Crabtree effect: A regulatory system in yeast, *Journal of General Microbiology* (1) (1966) 149–156.
- [42] X. C. Zhang, A. Visala, A. Halme, P. Linko, Functional state modelling approach for bioprocesses: Local models for aerobic yeast growth processes, *Journal of Process Control* 4 (3) (1994) 127–134. doi:10.1016/0959-1524(94)85004-6.
- [43] W. Woehrer, M. Roehr, Regulatory aspects of bakers’ yeast metabolism in aerobic fed-batch cultures, *Biotechnology and Bioengineering* 23 (3) (1981) 567–581. doi:10.1002/bit.260230308.

- [44] P. Dantigny, A. Guilmart, F. Radoi, M. Bensoussan, M. Zwietering, Modelling the effect of ethanol on growth rate of food spoilage moulds, *International Journal of Food Microbiology* 98 (3) (2005) 261–269. doi:10.1016/j.ijfoodmicro.2004.07.008.
- [45] Habegger, Loïc and Crespo, Kelly Rodrigues and Dabros, Michal, Preventing overflow metabolism in crabtree-positive microorganisms through on-line monitoring and control of fed-batch fermentations, *Fermentation* 4 (3). doi:10.3390/fermentation4030079.
- [46] Brignoli, Yann and Freeland, Brian and Cunningham, David and Dabros, Michal, Control of specific growth rate in fed-batch bioprocesses: Novel controller design for improved noise management, *Processes* 8 (6). doi:10.3390/PR8060679.
- [47] Butkus, Mantas and Repšyte, Jolanta and Galvanauskas, Vytautas, Fuzzy logic-based adaptive control of specific growth rate in fed-batch biotechnological processes. A simulation study, *Applied Sciences (Switzerland)* 10 (19). doi:10.3390/app10196818.



Highlights

- *Rhizopus oryzae* was grown without any liquid metabolite by-products.
- Feed addition was controlled at a fixed respiration quotient.
- Biomass yield was increased 3.3 times when compared to batch fermentation.
- The Crabtree effect was successfully utilised.
- Better understanding of *Rhizopus oryzae* as biocatalyst was achieved.

Conflicts of interest

The authors do not declare any conflicts of interest.

Funding

This work was supported by the University of Pretoria and by the CSIR Inter-bursary Programme, South Africa. **Opinions expressed are those of the author and not necessarily attributed to the CSIR.** The funding sources were not involved in the study, **in the** design, in the collection, analysis and interpretation of data, **in the writing of the report** and in the decision to submit the article for publication.

CRedit author statement

Nico de Jongh: Conceptualisation, Methodology, Software, Validation, Formal analysis, Investigation, Resources, Data Curation, Writing - Original Draft, Writing - Review & Editing, Visualization, Project administration, Funding acquisition

Reuben Swart: Software, Investigation, Resources

Willie Nicol: Conceptualisation, Validation, Resources, Writing - Review & Editing, Supervision, Project administration, Funding acquisition